Experiments with T-mesh for Constructing Bifurcation and Multi-furcation using Periodic Knot Vectors

Kritika Joshi[1] and Amba D. Bhatt[2]

[1]MNNIT, Allahabad, India, rme1615@mnnit.ac.in
[2]MNNIT, Allahabad, India, abhatt@mnnit.ac.in

Corresponding author: Amba D. Bhatt, abhatt@mnnit.ac.in

ABSTRACT

T-splines are now being increasingly used for design and analysis. However, there is a paucity of literature for the construction of closed and continuous surfaces especially bifurcations and multi-furcations using periodic T-Splines. This paper is an effort to experiment with T-splines and provide a clearer view to construct smooth bi-furcating and multi-furcating surfaces. These surfaces may be either open or closed surfaces. The results are encouraging and the experimentations provide the insight of the T-spline surface.

Keywords: T-spline, T-mesh, Bifurcation, Multi-furcation, Surface Construction.
DOI: https://doi.org/10.14733/cadaps.2019.382-395

1. INTRODUCTION

In recent years, surface modeling of the branched surfaces is widely applied in various fields of biomedical industry. These applications make use of scanned data set of the original object and reconstruct a new or modified version of the same object as per the design requirement. Mathematical models of bifurcating and multi-furcating surfaces are used in flow modeling of the cardiovascular and bronchial system [10] and also find its application in study and treatment of diseased coronary arteries [8]. Vukicevic et al. [14] used NURBS as a tool to increase the efficiency of XRA (X-ray angiography) procedure for the quantitative analysis of coronary arteries. Besides of all these biomedical applications, branched surface models are also used in automobile industry for design and analysis of engine manifold systems.

1.1 Previous Related Work

The construction of the branched surface faces complexities against best topological relation between adjacent contours, to maintain the geometrical continuity at junction [11]. In past, different

techniques have been used for preserving shape and continuity of the branched object upto certain level. Some initial attempts for the construction of bifurcating surface include the method of triangulation [9], joining of right circular cylindrical surfaces [5] and merging of half tubular Bezier patches [15]. These methods could not meet easily with the desired requirements of continuity and control over the surfaces. Although B-spline offers additional control over the surface through knot vectors unlike Bezier surface but the involvement of T-spline that allows a row of control point to terminate at an appropriate position, increases the flexibility of the surface with relatively less number of control points [12]. One possible solution to achieve the same quality of the surface is by merging of two or more B-spline surfaces of different knot vectors through T-spline [7],[12]. Ginnis et al [6] proposed an algorithm, which combined the concept of T-spline surface, surrounding curve and Euclidean Voronoi diagram, to generate one to many branching surface. These methods are good in the sense that smooth surface could be constructed however they lack the flexibility and speed of a single T-spline equation to construct such surfaces.

The concept of the disjoint surface for generating branched object was explained by Bhatt et al. [3]. They used B-spline surface representation to developed bifurcating surfaces. A similar method for constructing disjoint surfaces was developed by Asthana et al. [1]. They constructed an iterative procedure to develop multiple bifurcating surface models. The model developed by [1] was capable of handling any order of B-spline surfaces in both of the defining directions along with G1 continuity, which was maintained by aligning the control polygon segment in a straight line. In case of T-spline surfaces, continuity can be achieved by allowing local refinement in the corresponding T-mesh hence the absence of local refinement is considered as a major constraint while working with the B-spline based surface model. The present work therefore is an effort towards describing a complex surface with the help of a single T-spline surface equation.

1.2 Overview of this Paper

A bifurcating surface can be obtained by joining of one contour of i^{th} plane with two adjacent contours of $(i+1)^{th}$ plane depicted in Fig. 1. Whereas for multi-furcating surface one or both contours of $(i+1)^{th}$ plane behaves as a parent section, connected through adjacent contours of $(i+2)^{th}$ plane and so on.

The Continuity of the parametric curves in T-spline surfaces are characterized by the set of independent knot vectors unlike B-spline and NURBS where set of global knot vector define the whole domain of the surface. The T-spline surface is a point-based spline, where basis function is defined for every vertex of T-mesh. The structure of the T-mesh is based upon the complexity of the desired surface. Local refinement in T-mesh, allows sharp change in a small region of the surface, if required.

Here we put an effort to build a single T-mesh for bifurcating and multi-furcating surface which can further assist for surface fitting of branched object.

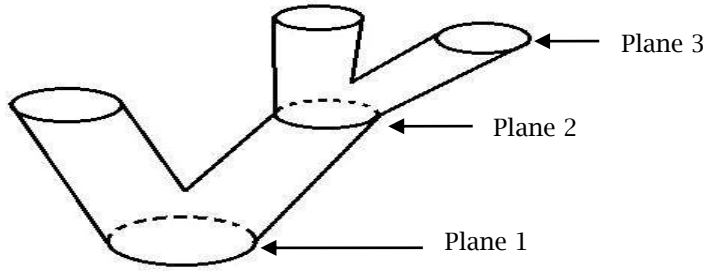

Figure 1: Representation of Branched Object by Joining of Planner Contour/s.

This work illustrates generation of bi-furcating and multi-furcating surface models by performing some experiments on T-mesh templates through local refinement at the required positions of the corresponding T-mesh. A presumed set of coordinates have been used which acts as control points for the generation of T-spline surface.

Construction of a T-mesh is based on the arrangement of control points, used to define the shape of the desired surface. In section 2, the methodology to generate a closed and disjoint T-spline surface (Stem and branched part) has been explained.

2 METHODOLOGY

The work started with a pre-assumed set of control points, through which a control polyhedron is made for an open bifurcating surface, closed bifurcating or multi-furcating surface as the case may be. It may be noted that for a real world problem, control polygon is derived from a real data set obtained from the concerned object.

To generate a T-spline surface, T-mesh is used as a two-dimensional pre-image of control polyhedron. It is a rectangular grid where each edge of every rectangle represents a positive integer value termed as knot value. For a given T-mesh of order k and each control point P_i having associated weight $w_{i,}$, the points on the T-spline surface $S(u,v)$ can be evaluated by the equation:

$$S(u,v) = \frac{\sum_{i=1}^{N} w_i P_i B_i(u,v)}{\sum_{i=1}^{N} w_i B_i(u,v)} \tag{2.1}$$

Where B_i (u,v) are tenser products of univariate B-spline basis function given by:

$$B_i(u,v) = N_{i,k}(u).N_{j,k}(v) \ , \quad (u,v) \in D \tag{2.2}$$

In a T-mesh, (u, v) represent knot coordinates for the anchor assigned as control points and D is the effective parametric domain to define a surface [12]. For odd degree polynomial each vertex of the T-mesh acts as a control point, and for even degree polynomial control point is considered to lie at the center of each rectangle of the T-mesh. Evaluation of the set of local knot vectors in both directions, for odd and even degree polynomial is explained by Bazilevs et al. [2].

2.1. Periodic T-mesh and Knot Vectors

Construction of a T-mesh is based on the number of control points in each plane of control polyhedron (including repeated control points if any). One can insert or remove control points from T-mesh to maintain the shape of the surface according to the rule described in previous works [13].

The concept behind a periodic T-spline surface is same as that of B-spline surface or NURBS. However, a T-spline surface offers additional control due to local refinement. In order make a closed surface, first and last control points should be same with k-2 number of repeated control points, as shown in Fig. 2. For a given control polyhedron, the number of control point will increase with order of the surface. Knot vector referring the first and last control point of the supporting parametric domain D, must have same knot interval to make this surface close, otherwise it will create overlapping or open surfaces. The parametric domain of the surface in u and v direction is considered as u_{min} to u_{max} and v_{min} to v_{max} respectively. The knot value assigned to the parametric domain is determined by arrangement of control points in T-mesh and order of the surface.

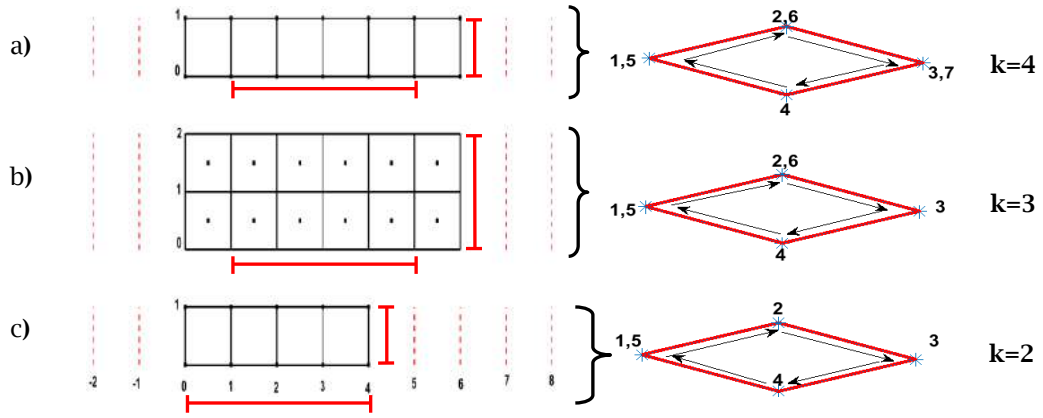

Figure 2: T-mesh of a Closed Surface, using Periodic Knot Vectors and First Row of Control Polygon (Right): (a) T-mesh and Control Polygon for Order k=4, (b) T-mesh and Control Polygon for Order k=3, (c) T-mesh and Control Polygon for Order k=2.

In the above example, where for k=2, minimum 5 control points are required to make a closed surface (as first and fifth control point are same) as shown in Fig. 2(c). While for k =3 and k=4, one and two control points have been repeated respectively as shown in Fig. 2(b) and Fig. 2(a).

2.2 Generation of Closed Disjoint T-spline Surface

The methods to generate disjoint B-spline surface has already been described previously [1]. The method of uni-directional disjoining through T-spline has been explained, to define the branched part of the surface. The repetition of the control point at the point of disjoining will depend upon the order of the surface. Fig. 3 shows two rows of a T-mesh (with respect to odd and even order) through which disjoining of the surface have been done.

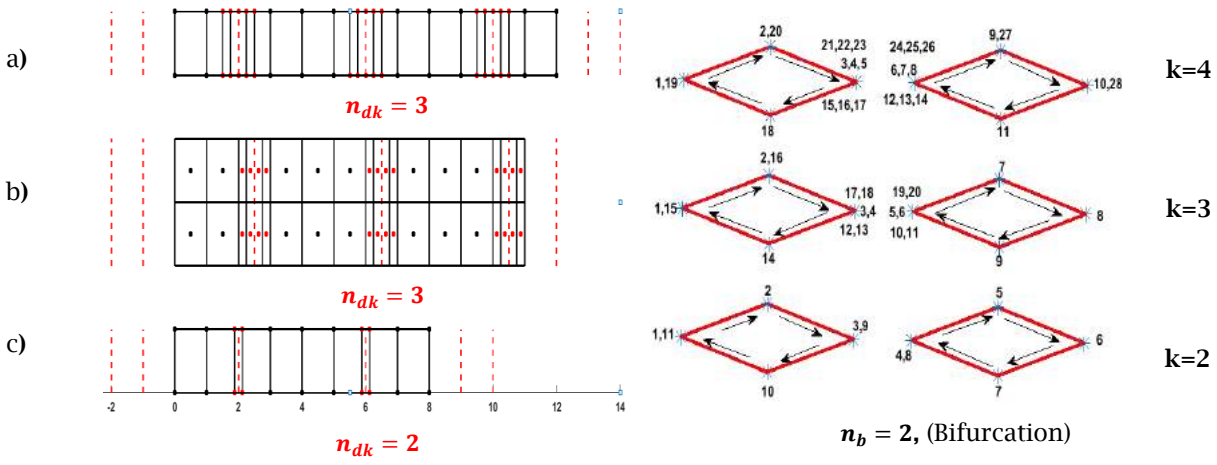

Figure 3: T-mesh to make Disjoint Surface using Periodic Knot Vectors and corresponding Sectional View of Control Polygon (Right): (a) T-mesh and Control Polygon for Order k=4, (b) T-mesh and Control Polygon for Order k=3, (c) T-mesh and Control Polygon for Order k=2.

Multiplicity of the control point has been done for three reasons. First one is to maintain periodicity as mentioned in sub-section 2.1, to create junction and the third reason is for disjoining of the surface. The number of disjoining points for bifurcation (n_{dk}) in a T-mesh has been decided by order of the surface. In case of multi-furcation, the total number of disjoining points (N_{dk}) could be determined using n_{dk} and number of control polygon used in first plane of control polyhedron (n_b). The generalized rule for multiplicity of the control points and knot value with respect to odd and even order of the surface has been given in sub-section 2.3.

In Fig. 3, control points represented by red dots in T-mesh are repeated number of the control point for disjoining the surface. If m_{cd} is the multiplicity of the control point at disjoint, then:

For k=2, $m_{cd} = 1$, P_3 and P_4 are point of discontinuity (Fig. 3(c)).

For k=3, $m_{cd} = 2$, $P_3 = P_4$ and $P_5 = P_6$ are point of discontinuity (Fig. 3(b)).

For k=4, $m_{cd} = 3$, $P_3 = P_4 = P_5$ and $P_6 = P_7 = P_8$ are point of discontinuity (Fig. 3(a)).

2.3 Generalized Rule to Create Bifurcating and Multi-furcating Surface through T-spline

In this sub-section, some generalized relations have been developed through observations which are based on experimental results. These relations are employed to create T-mesh for the respective branched surface. The construction of a two dimensional (u for x-axis and v for y-axis) T-mesh is done from a pre-defined control polyhedron. This T-mesh is divided into three parts in v-direction which are branched part, junction and stem part. To create junction the multiplicity of the control point has been taken as k in control polygon. Each repeated control point carries different knot vector corresponding to the T-mesh.

Under a specified domain, moving towards v direction will cause generation of curves along u direction. Input data is given as:

- Same order k in both of the parametric direction.
- x, y, z coordinates of the control points, represented by $P_{i,j}$ in the corresponding T-mesh.
- Number of planes h, containing control polygon/s (equal to number of rows in T-mesh), along v direction. Here h is the plane of minimum number of control points. The condition for the least number of plane in v direction is:

$$h_{min} > \text{ k}$$

If the number of control points in i^{th} plane is represented by n_i, total number of control point in T-mesh can be written as :

$$N = \sum_{i=1}^{h} n_i \tag{2.3}$$

The set of local knot vectors for each control point of T-mesh are inferred by shooting ray method [2]. The generalized set of local knot vector in u and v direction in absence of disjoining are:

$$\left(T_{i,j}^{loc}\right)_u = \{t_{j+m}\}_{m=0}^{k} \qquad 1 \le i \le h$$

$$\left(T_{i,j}^{loc}\right)_v = \{t_{i+m}\}_{m=0}^{k} \qquad 1 \le j \le n_i$$

In order to separate the two contours, multiplicity of the knot value (m_{kd}) at the end and start of the knot vectors, corresponding to the disjoining points (two different control point with same knot value in T-mesh) should be same as the multiplicity of control point (m_{cd}):

- For even order (k >2) $m_{kd} = \frac{k}{2} + 1 = m_{cd}$
- For odd order $m_{kd} = \frac{k+1}{2} = m_{cd}$

In case of k=2, multiplicity of control point and knot value has been taken as one. The repeating pattern of the control points for disjoining may vary according to the order and number of branching in the surface. For 2^{nd} order, single bifurcation, the number of disjoining points are two, referred in Fig. 3 and for k^{th} order it may be assumed as n_{dk}.

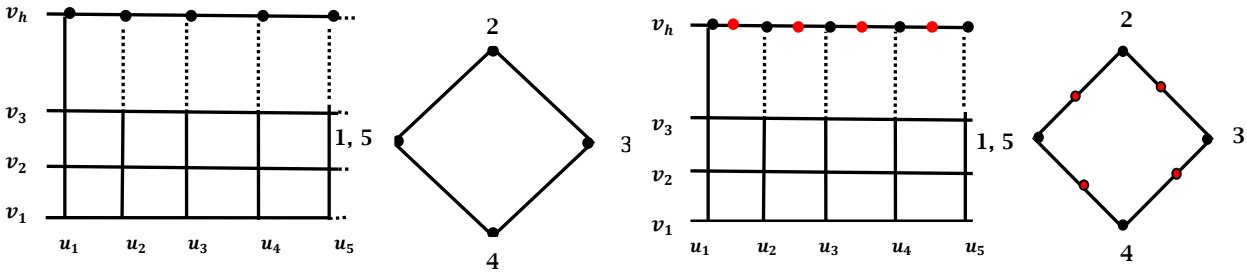

Figure 4: A T-mesh Focusing h^{th} row and corresponding Control Polygon: (a) T-mesh and its Control Polygon of Minimum Number of Control Points (Black), (b) T-mesh along with an Additional Control Point (Red) n_e, within Each Knot Span and its Control Polygon.

Let us consider the h^{th} row of the T-mesh, depicted in Fig. 4(a), corresponding to stem part of the control polyhedron, which uses minimum five number of control points to make a closed surface. Since the surface is closed in horizontal direction, the parametric values u_{min} and u_{max} could be corresponding to the control points (CP) P_{min} and P_{max}. Consider Fig. 4(a) and Tab. 1 to determine the parametric domain in u-direction, the generalized relations for P_{min} and P_{max} has been given by Eqn. 2.4 and Eqn. 2.5. The number of control point in h^{th} row can be taken as:

$$n_h = n_{min} + (k-2)$$

$n_{min} = 5$	Even order			Odd order	
order →	k=2 ($n_{min} = n_h$)	k=4	k=6	k=3	k=5
n_h	5	7	9	6	8
$(P_{min})_u$	1^{st} CP	2^{nd} CP	3^{rd} CP	2^{nd} CP	3^{rd} CP
u_{min}	u_1	u_2	u_3	u_2	u_3
$(P_{max})_u$	5^{th} CP	6^{th} CP	7^{th} CP	6^{th} CP	7^{th} CP
u_{max}	u_5	u_6	u_7	u_6	u_7

Table 1: Parametric Domain u_{min} and u_{max}, for k^{th} Order in Horizontal Direction.

For even order

$$(P_{min})_u = n_{min} - \left[n_{min} - \frac{k}{2}\right] \text{ and } (P_{max})_u = n_h - \left[\frac{k}{2} - 1\right] \quad (2.4)$$

$$v_{min} = v_1 \text{ and } v_{max} = v_h$$

$$n_{dk} = 2 + \frac{k-2}{2}$$

For odd order

$$(P_{min})_u = n_{min} - \left[n_{min} - \frac{k+1}{2}\right] \text{ and } (P_{max})_u = n_h - \left[\frac{k-3}{2}\right] \quad (2.5)$$

$$v_{min} = v_1 \text{ and } v_{max} = v_h$$

$$n_{dk} = 2 + \frac{k-1}{2}$$

In presence of n_e number of additional control points within each knot span as shown in Fig 4(b), control point $(P_{min})_{au}$ and $(P_{max})_{au}$ can be determined for both even and odd order by:

$$(P_{min})_{au} = (P_{min})_u + n_e((P_{min})_u - 1)$$
$$(P_{max})_{au} = (P_{max})_u + n_e((P_{max})_u - 1)$$

The number of knot added within each knot span should be same. For one control point added in each knot span, n_e =1. If n_b is the number of control polygon employed in first row of the T-mesh, disjoint points in T-mesh can be given by:

$$N_{dk} = n_{dk}(n_b - 1)$$

By employing these relations for T-mesh, the final surface could be obtained using definition of T-spline surface, given in Eqn. 2.1. The above relations are valid for serial bifurcation (extension of bifurcation into multi-furcation).

3 DISCUSSIONS ON EXPERIMENTS

Experiments are carried out to form bifurcating and multi-furcating surfaces. Initially, T-mesh has been constructed for a simple open bifurcating surface. Although surfaces discussed in this section can be extended to any polynomial degree but most of the surfaces are generated through series of experiments performed on T-mesh having order k=4 in both of the parametric direction.

3.1. Control Polyhedron Representation For Closed Surface

The construction of control polyhedron is based on the shape of the desired surface. The control point layouts presented by Fig. 5, gives the geometrical arrangement of control points in parallel horizontal planes along the y-axis, forming rhombus shapes (either one or more) is referred to as a control polygon for that plane. These number of plane of control polygons, are equal to the number of rows in the corresponding T-mesh. The points lying in a control polygon decide the arrangement of knots (equal to the number of control points) in that row of T-mesh. The desired bifurcating surface can be created in three different ways. These layouts have been utilized and discussed further to construct T-meshes and corresponding surfaces.

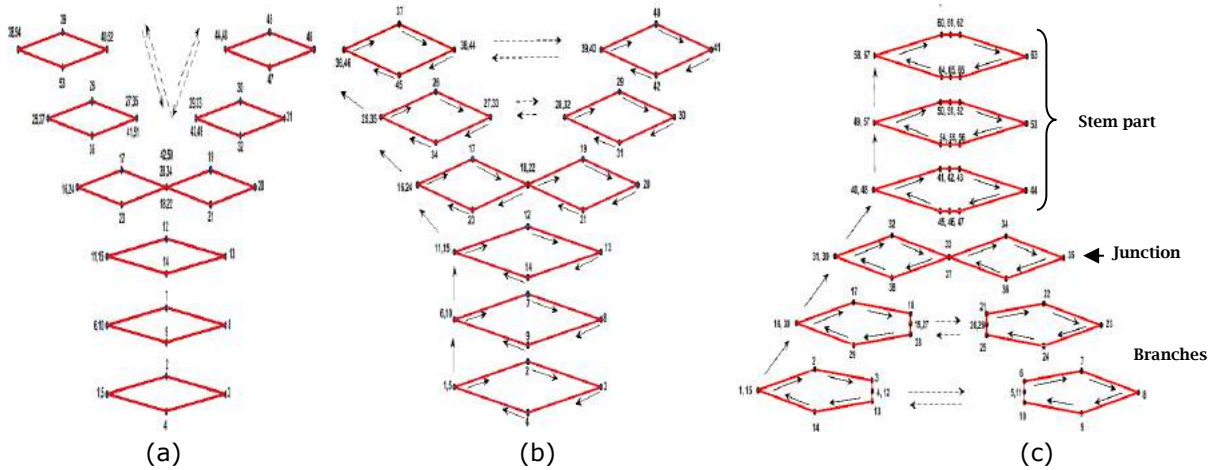

Figure 5: Three Ways for Arrangement of Control Point in a Control Polyhedron of Bifurcating Surface: (a) Separation of Two Branches without Disjoining Technique, (b) Separation of Two Branches with Disjoining Technique, (c) Inverted Arrangement of Control Points.

The pattern of the control points in the control polyhedron has been shown in Fig. 5. However, the multiplicity of control points required to generate close and disjoint surface have not been depicted these figures. All the branching surfaces illustrated, have been generated by following one of these three patterns and will be discussed in upcoming subsections. The shape of the control polygon can be altered by adding control points, but the overall layout of the control polyhedron will remain same.

3.2. Open and Closed Bifurcating T-spline Surface

This subsection shows the T-mesh and corresponding surfaces which follow the layout of control polyhedron, displayed in Fig. 5 and utilize the methodology described in section 2.

3.2.1 Open bifurcating surface

The surface shown in Fig. 6 has been constructed by considering the same pattern of control point displayed in Fig. 5(a). However for open surface, control points have been removed from the layout in negative z-direction. The layout has been developed by to and fro repetition of the control point through the junction of the bifurcating surface. For each repeated control point, knot coordinates in T-mesh is different and can be determine from Fig. 6(a). Each vertex of T-mesh represents control point having knot coordinates (u, v). In order to create junction and branches, control point has been inserted in the T-mesh shown in Fig. 6(a). The repetition enables the surface to pass through the desired control point however this will degrade the continuity of the surface.

3.2.2 Closed bifurcating surface

The design of the closed bifurcating surface from first two arrangements of control points, illustrated by Fig. 5(a) and Fig. 5(b) has been addressed in this part. To achieve this, periodic knot vectors has been adopted in the definition of T-spline surface as given in Eqn. 2.1. The Layout of the control point shown in Fig. 5(a) has been taken to plot the T-mesh and corresponding surface, displayed in Fig. 7(a) and Fig. 7(b) respectively. The obtained closed surface is dominated by back and forth repetition of the control point to disjoint the branches from stem part, which results multiple parametric lines converged at the junction and are clearly visible in Fig. 7(b).

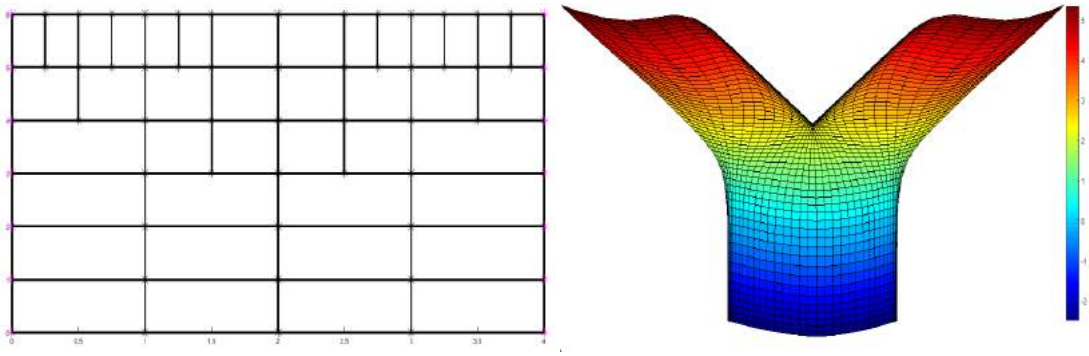

(a) (b)

Figure 6: T-mesh (order k=4) and corresponding Open Bifurcating Surface using Pattern of Control Polyhedron Shown in Fig. 5(a): (a) T- mesh used for Construction, (b) Resulting Bifurcating Surface.

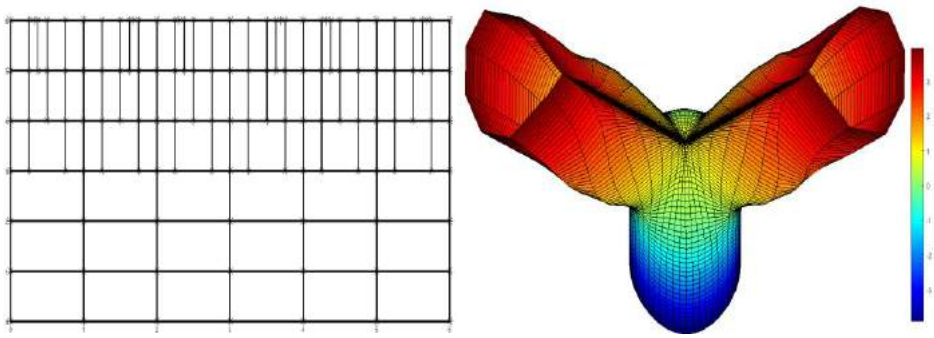

(a) (b)

Figure 7: T-mesh (order k=4) and corresponding Closed Bifurcating Surface using Control Polyhedron Shown in Fig. 5(a): (a) T- mesh used for Construction, (b) Resulting Closed Bifurcating Surface.

k=4,	Fig. 6	Fig. 7	Fig. 8	Fig. 9
N	61	157	124	163
h	7	7	7	7
u_{min} to u_{max}	0 - 4	1 - 5	1 -5	2-10
v_{min} to v_{max}	0 - 6	0 - 6	0 - 6	0 - 6

Table 2: Data Utilized by Open and Closed Surfaces Shown in Fig. 6, Fig. 7, Fig. 8 and Fig. 9 Respectively.

The surface displayed in Fig. 8(b) has been made to minimize the multiple parametric lines which are visible due to continuous repetition of control point as mentioned previously. In this approach, two parallel contours in branched part are separated by method of disjoining, as shown in Fig. 5(b). Methodology to generate closed disjoint surface from a T-mesh has already been addressed in sub-section 2.2. In Fig. 5(b), minimum number of the control point has been utilized (started from stem part) to decide knot interval in the first three rows of the corresponding T-mesh shown in Fig. 8(a), after that knots have been inserted in order to create junction and branched part respectively. Newly acquired closed bifurcating surface as shown in Fig. 8(b) is smooth, continuous at the junction and carrying relatively less number of control points (Tab. 2) as compared to Fig. 7(b).

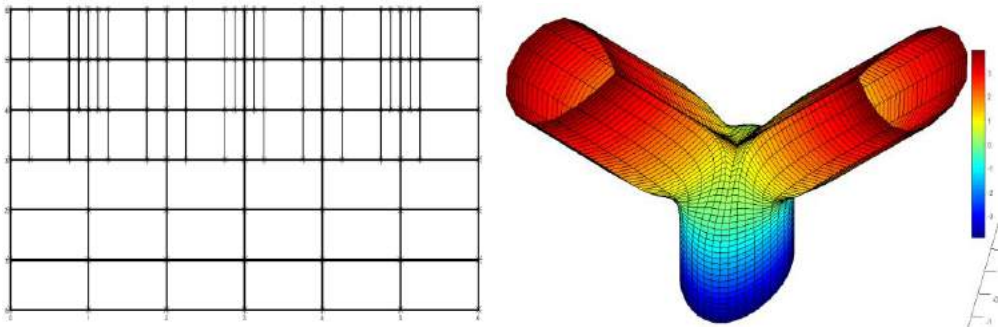

(a) (b)

Figure 8: T-mesh (order k=4) and corresponding Closed Bifurcating Surface using Control Polyhedron Shown in Fig. 5(b): (a) T- mesh used for Construction, (b) Resulting Closed Bifurcating Surface.

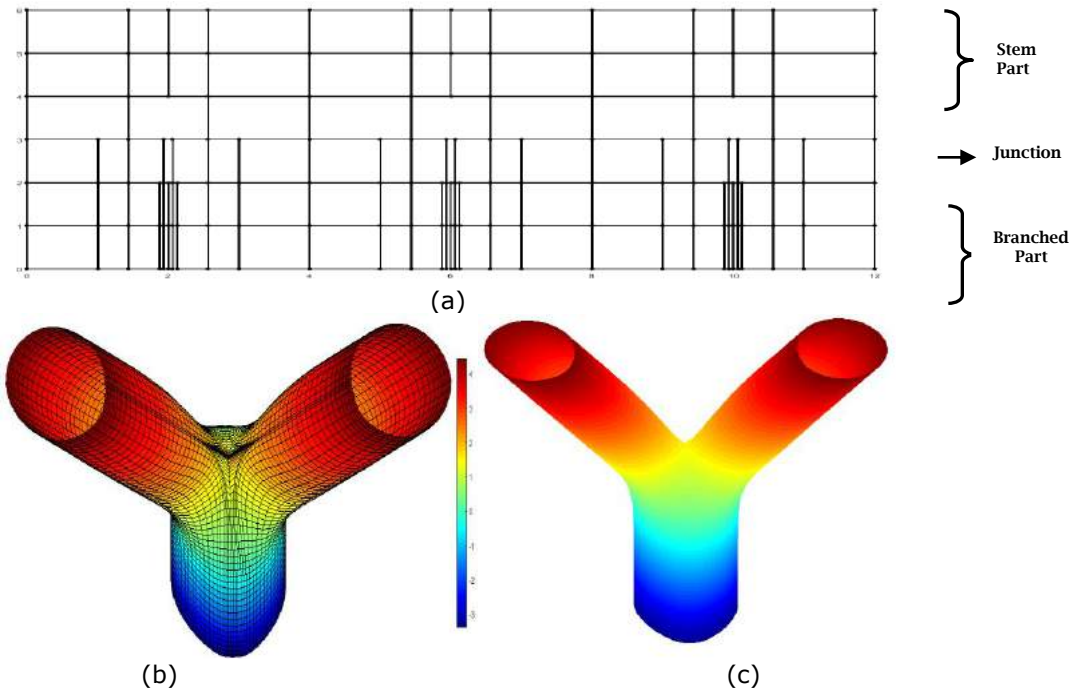

Figure 9: T-mesh (order k=4) and corresponding Closed Bifurcating Surface using Control Polyhedron Shown in Fig. 5(c): (a) T- mesh used for Construction of the Surface, (b) Resulting Bifurcating Surface, (c) Closed Bifurcating Surface with Interpolating Shading.

3.2.3 Closed bifurcating surface using final control polyhedron

This part introduced final layout shown in Fig. 5(c), and corresponding T-mesh illustrated in Fig. 9(a). The relations given in sub-section 2.3, has been developed by considering the final layout to construct branching surfaces. Even though the bifurcating surfaces, obtained by employing the layouts, Fig. 5(b) and Fig. 5(c) are quite similar and shown by Fig. 8(b) and Fig. 9(b), still inverted (first row of T-mesh is taken from the branched part of the surface) arrangement of control points given by Fig. 5(c) has been found more convenient for multi-furcating surfaces. In case of multi-furcating surface, maximum number of control point can be utilized as knot values in the first row of the T-mesh.

While addressing a branched surface model, the number of control points has been increased as one move from stem to branched part. Extra control points have been added, to reduce the sharpness at the edges of the branches. To achieve the surface shown in Fig. 9(b), knot interval in the first three rows of the T-mesh, has been decided according to the branched part of the layout shown in Fig. 5(c) unlike previous one in which knot interval was decided according to stem part of the layout Fig. 5(b). The range of parametric value will increase with the number of control polygon used in branch part (for multi-furcating surfaces).

3.3 Closed Multi-furcating T-spline Surfaces

The method for constructing bifurcations using final layout, is further extended to multi-furcations. In order to maintain the flexibility of the T-mesh in multi-furcation, similar pattern of the control points have been incorporated with the method of disjoining.

3.3.1 Asymmetric and symmetric closed multi-furcating surface

When the number of branches evolved from parent branch is same then it is called symmetrical branching. The surface shown in Fig. 12 is an example of a closed symmetrical branched surface and when number of branches evolved are not same as shown in Fig. 11, is called a asymmetrical branched surface. The methodology employed to construct both of the surfaces are same but in asymmetric branching, the way of assigning knot interval in T-mesh has been changed shown in Fig .10. This change has been done to keep the same knot interval for the control points (corresponding to the supporting parametric domain) used to close the surface in their set of local knot vector.

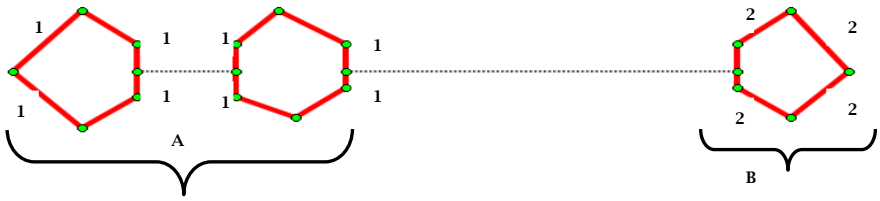

Figure 10: Sectional View of the Control Polygon used to make first row of the T-mesh of a Closed Asymmetrical Surface Shown in Fig. 11.

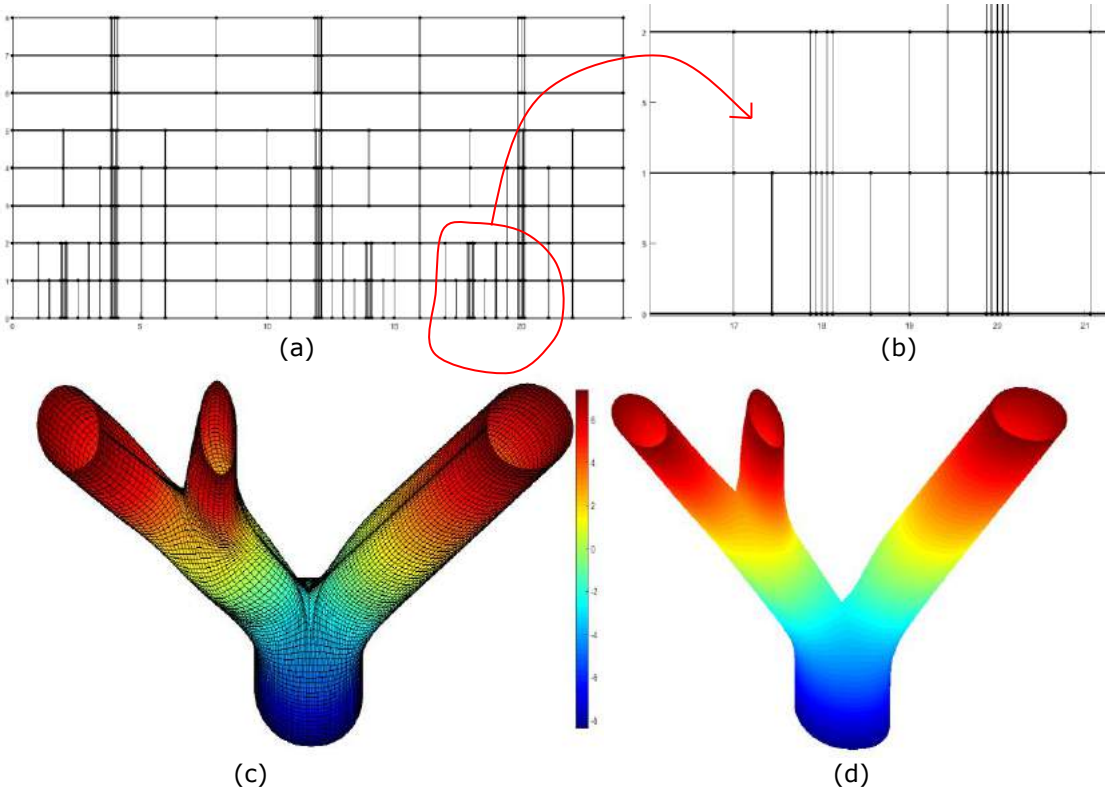

Figure 11: T-mesh (order k=4) and corresponding Asymmetrical Closed Multi-furcating Surface: (a) T- mesh used for the Construction of the Surface, (b) Enlarged View of Circled Part of T-mesh, (c) Resulting Multi-furcating Surface, (d) Closed Multi-furcating Surface with interpolating shading.

Fig. 10 gives the idea of sectional views of the three control polygon lies in the first plane of control polyhedron (similar to Fig. 5(c)). In order to preserve closeness of the surface, the knot values

for control points that lie within A and B has been arranged in such a way that it can achieve equal knot interval with respect to the local knot vector of the closing control points.

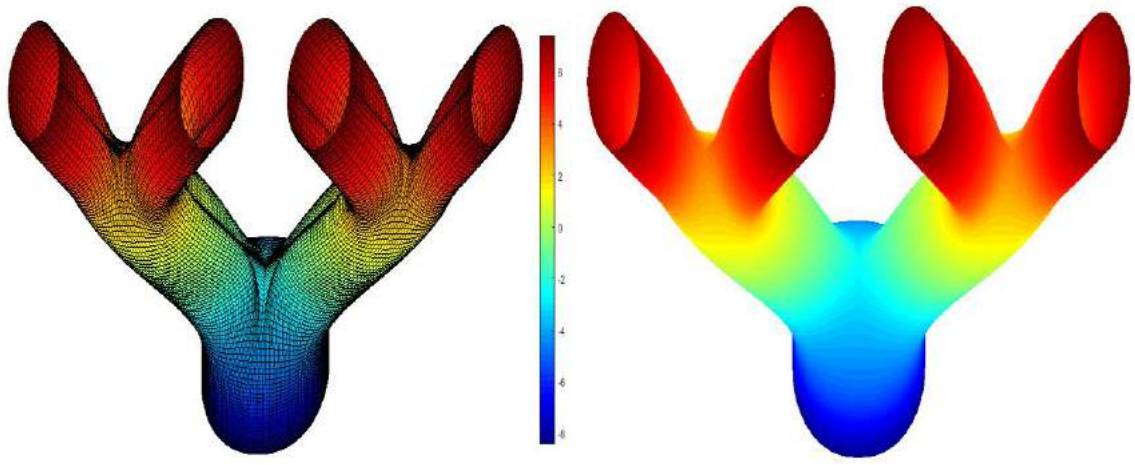

(a) (b)

Figure 12: Symmetrical Multi-furcating Surface (order k=4): (a) Resulting Multi-furcating Surface, (b) Closed Multi-furcating Surface with Interpolating Shading.

To design a multi-furcating surface, control polygon in the first plane may vary according to the branches required in the higher generation of the surface. For a simple bifurcating surface, the number of control polygon in the first plane has been taken as two shown in Fig. 3(a) and the number of control points in the first row of T-mesh varies accordingly. The surface shown in Fig. 12(a) is a symmetric multi-furcating surface in which four control polygons has been used in the first plane of control polyhedron. Same number of control polygon has been used in tri-furcation shown in Fig. 13.

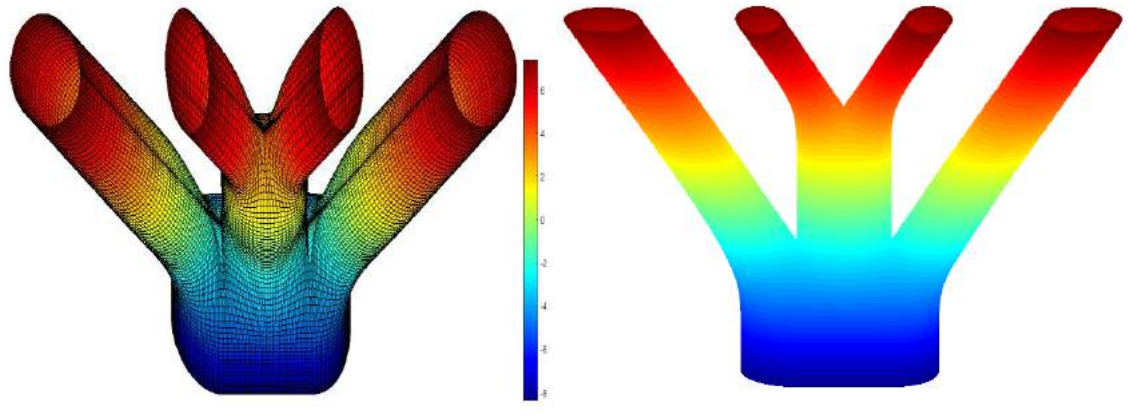

(a) (b)

Figure 13: Tri-furcating Surface (order k=4): (a) Tri-furcating Surface in Parametric Space, (b) Closed Tri-furcating Surface with Interpolating Shading.

K=4,	Fig. 11	Fig. 12	Fig. 13

N	300	369	429
h	9	9	9
u_{min} to u_{max}	4 - 20	4 - 20	4 - 28
v_{min} to v_{max}	0 - 8	0 - 8	0 - 8

Table 3: Data Utilized by Multi-furcating Surfaces, Shown in Fig. 11, Fig. 12, and Fig. 13 Respectively.

The range of parametric domain in u-direction will be more in case of trifurcation since three branches evolved from stem part of the surface.

4 COMPARISON OF LAYOUTS FOR CONSTRUCTION OF BRANCHING SURFACE

The results of experiments performed on the arrangement of control points and corresponding T-meshes has been discussed in the previous section. Extension of the first layout (Fig. 5(a)) to make multi-furcating surface has been aborted due to complexity in the repetition of control points and discontinuities obtained in resulting bifurcating surface.

Use of the second layout (Fig. 5(b)) has been found simple for the construction of bifurcating surface through T-mesh. In the first row of T-mesh, knot values are placed according to the control point in stem part (minimum number of control points). As one move from stem to branched part knots are inserted in between the previously assigned knots to get the desired shape. In case of the multi-furcating surface when control point has been increased, it becomes difficult to insert more control points in between previously assigned knot values.

The final model of the control polyhedron (Fig. 5(c)) has been found more appropriate for the extension of bifurcation into multi-furcating surface. In final layout, knots have already been assigned according to the maximum number of control points (branched part), thus to maintain the shape of the surface one need to remove control points as moving away from the branched part.

Although the method to create bifurcation is same in both second and third layout but the construction of T-mesh from the third layout has been found good enough to achieve the required closed, multi-furcating surface.

5 CONCLUSIONS

In the present work, some experiments have been performed on T-mesh templates to construct bifurcations and multi-furcations. These experiments show that use of disjoint surface in periodic T-spline is an effective method to construct smooth and continuous branched surface. However, in case of multi-furcation, it is difficult to maintain the flexibility of the T-mesh for upper level branching with respect to the lower level bifurcation. This problem can be resolved by altering the T-mesh according to the pattern of control point shown in the final layout. These methods can be applied in applications where smooth reconstruction of bifurcating or multi-furcating part is required.

Kritika Joshi, http://orcid.org/0000-0002-1622-8785
Amba D. Bhatt, http://orcid.org/0000-0003-0022-1930

REFERENCES

[1] Asthana, V.; Bhatt, A.-D.: G1 Continuous bifurcating and multi-bifurcating surface generation with B-spline, Computer-Aided Design & Applications, 14(1), 2017, 95-106. https://doi.org/10.1080/16864360.2016.1199759

[2] Bazilevs, Y.; Calo, V.-M.; Cottrell, J.-A.; Evans, J.-A.; Hughes, T.-J.-R.; Lipton, S.; Scott. M.-A.; Sederberg, T.-W.: Isogeometric analysis using T-splines, Computer Methods in Applied

Mechanics and Engineering, 199(5-8), 2010, 229-263. https://doi.org/10.1016/j.cma.2009.02.036
[3] Bhatt, A.-D.; Goel, A.; Gupta, U.; Awasthi, S.: Reconstruction of Branched Surfaces: Experiments with Disjoint B-spline Surfaces, Computer-Aided Design & Applications, 11(1), 2014, 76-85. https://doi.org/10.14733/cadconfP.2014.14-16
[4] Cardon, D.-L.: T-Spline Simplification, BYU Scholars Archive, Brigham Young University, Provo, Utah, 2007.
[5] Felkel, P.; Wegenkittl, R; Buhler, K.: Surface models of tube trees, Computer Graphics international, 2004, 70-77.
[6] Ginnis, A.-I.; Kostas, K.-V.; Kaklis, P.D.: Construction of smooth branching surface using T-splines, Computer-Aided Design, 92, 2017, 22-32. https://doi.org/10.1016/j.cad.2017.06.001
[7] Ipson, H.: T-SPLINE MERGING, BYU Scholars Archive, Brigham Young University, Provo, Utah, 2005.
[8] Jewkes, R.; Burton, H.-E.; Espino, D.-M.: Towards Additive Manufacture of Functional, Spline-Based Morphometric Models of Healthy and Diseased Coronary Arteries: In-Vitro Proof-of-Concept using a Porcine Template, Journal of Functional Biomaterials, 9(1), 2018, 15. https://doi.org/10.3390/jfb9010015
[9] Klein, R.; Schilling, A.; Strasser, W.: Reconstruction and simplification of surfaces from contours, Graphical Models, 62(6), 2000, 429-443. https://doi.org/10.1006/gmod.2000.0530
[10] Koullips, P.-G.; Kassinos, S.-C.; Bivolarova, M.-P.; Melikov, M.-K.: Particle deposition in a realistic geometry of the human conducting airways: Effects of inlet velocity profile, inhalation flowrate and electrostatic charge, Journal of Biomechanics, 49, 2016, 2201-2212. https://doi.org/10.1016/j.jbiomech.2015.11.029
[11] Meyers, D.; Skinner, S.; Sloan, K.: Surfaces from Contours, ACM Transactions on Graphics, 11(3), 1992, 228-258. https://doi.org/10.1145/130881.131213
[12] Sederberg, T.-W.; Zheng, J.; Bakenov, A.; Nasri, A.: N. L.: T-splines and T-NURCCs, ACM Transactions on Graphics, 22(3), 2003, 477-484. https://doi.org/10.1145/882262.882295
[13] Sederberg, T.-W.; Cardon, D.-C.; Finnigan, G.-T.; North, N.-N.; Zheng, J.; Lyche. T.: N. L.: T-splines Simplification and Local Refinement, ACM Transactions on Graphics, 23(3), 2004, 276-283. https://doi.org/10.1145/1015706.1015715
[14] Vukicevic, A.-M.; Cimen, S.; Jagic, N.; Jovicic, G.; Frangi, A.-F.; Filipovic, N.: Three-dimensional reconstruction and NURBS-based structured meshing of coronary arteries from the conventional X-ray Angiography projection images, Scientific Reports , 8(1), 2018, 1711. https://doi.org/10.1038/s41598-018-19440-9
[15] Ye, X.; Cai, Y.-Y.; Chui, C.; Anderson, J.-H.: Constructive modeling of G1 bifurcation, Computer Aided Geometric Design, 19(7), 2002, 513-531. https://doi.org/10.1016/S0167-8396(02)00131-0
[16] Zheng, J.; Wang, Z.: Periodic T-splines and Tubular Surface Fitting, Curve and Surfaces-ICCS 2010, Springer, Avignon, France, 2010.